

## RESEARCH ON HEAT TRANSFER CHARACTERISTICS AND BOREHOLE FIELD LAYOUT OF GROUND HEAT EXCHANGERS TO ALLEVIATE THERMAL ACCUMULATION WITH GROUNDWATER ADVECTION

by

**Zhongcheng SUN<sup>a,b</sup>, Zhixia HE<sup>b</sup>, and Mingzhi YU<sup>c\*</sup>**

<sup>a</sup> School of Energy and Power Engineering, Jiangsu University, Zhenjiang, China

<sup>b</sup> Institute for Energy Research, Jiangsu University, Zhenjiang, China

<sup>c</sup> School of Thermal Engineering, Shandong Jianzhu University, Jinan, China

Original scientific paper

<https://doi.org/10.2298/TSCI200822164S>

*The heat transfer performance of ground heat exchanger is significant to the ground source heat pump. The soil thermal parameters, the groundwater advection and the different borehole field layout are important factors to affect the performance of ground heat exchanger. Therefore, the influence of groundwater advection velocity, soil physical parameters and different borehole field layout on the soil temperature distribution and evolution around the ground heat exchanger has been analyzed and studied with unbalanced seasonal thermal load based on the moving finite line heat source model with groundwater advection. The results show that the heat accumulation is easy to occur as the time develops when the groundwater advection is taken into consideration. No matter what type of geological condition is employed, a reasonable borehole field layout can effectively avoid heat accumulation problems under the condition of keeping the same amount boreholes without changing the original ground area. The borehole field layout dispersed along the center line of the advection and concentrated in the advection downstream relatively can effectively reduce the heat accumulation.*

Key words: *ground heat exchanger, groundwater advection, borehole field layout, heat transfer, heat accumulation*

### Introduction

The advancement of geothermal energy utilization has evolved considerably in the past years [1, 2]. The ground source heat pump (GSHP) [3] is widely used in the field of building air conditioning with the renewable energy technology represented by geothermal energy, and it is gradually promoted. Many studies have been carried out to evaluate the performance of ground heat exchanger (GHE) including heating and cooling performance of GHE [4, 5], long-term running of GHE with unbalanced heating and cooling load [6, 7], and the effect on GHE performance of different parameters [8, 9]. However, groundwater advection, as an important factor, cannot be ignored in the design of boreholes in groundwater-rich areas [10, 11], which can easily cause the heat accumulation in long-term operation of GSHP system, especially for unbalanced seasonal load [12, 13]. According to the previous research, the main effective methods for solving the problem of thermal accumulation include enlarging

\* Corresponding author, e-mail: yumingzhiwh@163.com

the boreholes spacing [14], improving the GHE heat transfer efficiency by optimizing the GHE geometry or adding fins inside the pipe [15, 16], adopting a ground-coupled heat pump system [17, 18], and adopting zoning operation method [19]. However, enlarging boreholes spacing sometimes is restricted by the ground area, improving GHE heat transfer efficiency always increases initial costs and running fees, adopting coupled systems and zoning operation method usually makes the operation more complex. In consequence, this paper proposes a novel solution of changing the borehole field layout, which is applied effortlessly to diminish its ground thermal abnormalities without complex and expensive costs.

Analytical and numerical heat transfer models are used to analyze the effect of parameters like soil properties, borehole field layout, GHE heat transfer processes and building cooling or heating loads, *etc.* Molinagiraldo *et al.* [20] put forward the moving finite line source (MFLS) method to account for axial heat conduction effects, which takes groundwater advection into account. Cappa *et al.* [21] verified the moving infinite line source theory in a real case study and used it for boreholes heat transfer simulations. Besides, some numerical models were proposed [22, 23] with the aid of some simulation software such as the COMSOL multi-physics and the FLUENT, which can account for some complexities of the heat transfer problems. However, simulating the heat transfer process of a large GHE with many boreholes usually requires large numbers of grids and long calculating time during the calculating. The analytical methods are widely used in practical engineering to describe the soil temperature distribution around boreholes.

In this paper, we present several borehole field layouts to reduce the thermal accumulation of GHE by changing borehole field layout with unbalanced seasonal loads under groundwater advection. Firstly, the effect of soil thermal property parameters and advection velocity on the heat transfer performance of multi-boreholes is analyzed based on the MFLS model. Then, the soil temperature distribution and enthalpy increment of some borehole field layouts are compared with the normal uniform layout to find the most best borehole layout which mostly alleviates the thermal accumulation after long operation.

### **Mathematical model of heat transfer outside the multi-boreholes with groundwater advection**

The MFLS model was established based on the following assumptions: The soil is regarded as a homogeneous porous medium with constant thermal properties. The soil has a uniform initial temperature, and ground surface temperature maintains constant. The thermal contact resistance of boreholes can be neglected. The heat flow rate per unit length of the borehole remains constant values during the operational% periods. The ground advection velocity remains constant. All the materials properties related to the GHE are temperature independent and invariable.

As the diameter of the vertical borehole is much smaller than its depth, the heat transfer of the borehole is simplified to a MFLS in a semi-infinite medium. Under the condition of groundwater advection, the way of heat transfer in the soil included conduction through its solid matrix and liquid in its pores as well as convection of the moving liquid, the energy equation can be written as [24]:

$$\rho c \frac{\partial T}{\partial \tau} + \rho_w c_w u \nabla T = \nabla(\lambda \nabla T) \quad (1)$$

subjected to the initial and boundary conditions following [25]:

$$\begin{aligned}
 \tau \geq 0, \quad z = 0: T &= T_0 \\
 \tau = 0, \quad 0 < r < \infty: T &= T_0 \\
 \tau > 0, \quad r \rightarrow \infty: T &= T_0 \\
 \tau > 0, \quad r \rightarrow 0: -\lambda \frac{\partial T}{\partial r} 2\pi r' &= q_l
 \end{aligned} \tag{2}$$

where  $T$  [K] is the temperature,  $T_0$  [K] – the initial temperature,  $\tau$  [seconds] – the time,  $\rho c = \varphi \rho_w c_w + (1 - \varphi) \rho_s c_s$  [ $\text{Jkg}^{-1}\text{K}^{-1}$ ] which denotes the efficient specific heat capacity of underground soil,  $\varphi$  – the porosity of porous medium,  $\rho_w c_w$  and  $\rho_s c_s$  [ $\text{Jkg}^{-1}\text{K}^{-1}$ ] – the specific heat capacity of groundwater and underground soil, respectively,  $\lambda$  [ $\text{Wm}^{-1}\text{K}^{-1}$ ] – the efficient thermal conductivity of solid matrix and groundwater in the soil,  $\lambda = \varphi \lambda_w + (1 - \varphi) \lambda_s$  [ $\text{Wm}^{-1}\text{K}^{-1}$ ] where  $\lambda_w$  is the water thermal conductivity and  $\lambda_s$  the soil thermal conductivity,  $u$  [ $\text{ms}^{-1}$ ] – the velocity of groundwater advection,  $q_l$  [ $\text{Wm}^{-1}$ ] – the heating rate per length of source. In addition,  $r = (x^2 + y^2)^{1/2}$ ,  $r' = [r^2 + (2 - h)^2]^{1/2}$  [m]. Introduced the equivalent Darcy velocity,  $U = \rho_w c_w u (\rho c)^{-1}$  [ $\text{ms}^{-1}$ ], which is the effective heat transport velocity, and the thermal diffusivity of porous media,  $\alpha = \lambda (\rho c)^{-1}$ , [ $\text{m}^2\text{s}^{-1}$ ]. We can obtain the solution to the dynamic temperature variation at any point in the soil temperature field around a single borehole based on the fictitious line heat source and the Green's function method [26]:

$$\Delta T_{\text{MFLS}} = \frac{q_l}{2\pi\lambda} \exp \frac{Ux}{2a} \int_0^H \exp [f_1(x, y, z, \tau) - f_2(x, y, z, \tau)] dh \tag{3}$$

In which:

$$\begin{aligned}
 f_1(x, y, z, \tau) = \frac{1}{4\sqrt{r^2 + (z - h)^2}} \left\{ \exp \left[ -\frac{U\sqrt{r^2 + (z - h)^2}}{2a} \right] \text{erfc} \left[ \frac{\sqrt{r^2 + (z - h)^2} - U\tau}{2\sqrt{a\tau}} \right] + \right. \\
 \left. + \exp \left[ \frac{U\sqrt{r^2 + (z - h)^2}}{2a} \right] \text{erfc} \left[ \frac{\sqrt{r^2 + (z - h)^2} - U\tau}{2\sqrt{a\tau}} \right] \right\} \tag{4}
 \end{aligned}$$

$$\begin{aligned}
 f_2(x, y, z, \tau) = \frac{1}{4\sqrt{r^2 + (z + h)^2}} \left\{ \exp \left[ -\frac{U\sqrt{r^2 + (z + h)^2}}{2a} \right] \text{erfc} \left[ \frac{\sqrt{r^2 + (z + h)^2} - U\tau}{2\sqrt{a\tau}} \right] + \right. \\
 \left. + \exp \left[ \frac{v_T\sqrt{r^2 + (z + h)^2}}{2a} \right] \text{erfc} \left[ \frac{\sqrt{r^2 + (z + h)^2} - U\tau}{2\sqrt{a\tau}} \right] \right\} \tag{5}
 \end{aligned}$$

where  $\Delta T_{\text{MFLS}}$  [K] is the soil temperature variation at distance  $r$  from the center of borehole,  $h$  [m] – the length along the borehole depth,  $H$  [m] – the borehole depth, and erfc – the complementary error function. According to the superposition principle, the dynamic heat load in operation of boreholes is considered [27], and then the variable heat source theory [28] of boreholes is used to obtain the MFLS model of multi-boreholes, which can describe the temperature variation of any point at the soil temperature field around multi-boreholes. The expression can be written:

$$\Delta T(x, y, z, \tau) = \sum_{i=1}^n \sum_{j=1}^m \frac{q_{i,j} - q_{i,j-1}}{2\pi\lambda} \exp \frac{UX_T}{2a}$$

$$\cdot \int_0^H \exp[f_1(x, y, z, \tau_m - \tau_{j-1}) - f_2(x, y, z, \tau_m - \tau_{j-1})] dh \quad (6)$$

$$f_1(x, y, z, \tau) = \frac{1}{4\sqrt{r_i^2 + (z-h)^2}} \left\{ \exp \left[ -\frac{U\sqrt{r_i^2 + (z-h)^2}}{2a} \right] \operatorname{erfc} \left[ \frac{\sqrt{r_i^2 + (z-h)^2} - U\tau}{2\sqrt{a(\tau_m - \tau_{j-1})}} \right] + \right. \\ \left. + \exp \left[ \frac{U\sqrt{r_i^2 + (z-h)^2}}{2a} \right] \operatorname{erfc} \left[ \frac{\sqrt{r_i^2 + (z-h)^2} + U\tau}{2\sqrt{a(\tau_m - \tau_{j-1})}} \right] \right\} \quad (7)$$

$$f_2(x, y, z, \tau) = \frac{1}{4\sqrt{r_i^2 + (z+h)^2}} \left\{ \exp \left[ -\frac{U\sqrt{r_i^2 + (z+h)^2}}{2a} \right] \operatorname{erfc} \left[ \frac{\sqrt{r_i^2 + (z+h)^2} - U\tau}{2\sqrt{a(\tau_m - \tau_{j-1})}} \right] + \right. \\ \left. + \exp \left[ \frac{U\sqrt{r_i^2 + (z+h)^2}}{2a} \right] \operatorname{erfc} \left[ \frac{\sqrt{r_i^2 + (z+h)^2} + U\tau}{2\sqrt{a(\tau_m - \tau_{j-1})}} \right] \right\} \quad (8)$$

where  $i$  is the number of boreholes and the total number is  $n$ ,  $j$  – the number of time step and the total time step is  $m$   $q_{i,j}$  [ $\text{Wm}^{-1}$ ] – the heat flux at the  $j$  moment of the  $i^{\text{th}}$  borehole in the multi-boreholes,  $r_i = [(x - x_{ip})^2 + (y - y_{iq})^2]^{1/2}$  [m] – the distance from the calculating point to  $i^{\text{th}}$  borehole in the multi-boreholes, and  $X_T$  [m] – the distance from the calculating point to the  $i^{\text{th}}$  borehole along  $x$ -direction in the multi-boreholes,  $X_T = x - x_{ip}$ . In addition, the temperature of the boreholes at the center location is represented the mean temperature calculated by the both side of the borehole wall based on the above analytical solution.

### Analysis of multi-boreholes with groundwater advection during the operation

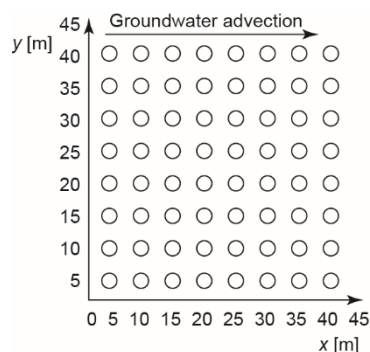


Figure 1. Layout of multi-boreholes

### The MFLS model for multi-boreholes

A region in size of  $45 \times 45 \times 100$  m, in which an  $8 \times 8$  m array of boreholes of 100 m in depth was constructed to simulate the heat transfer of the GHE, and the diameter of the boreholes is 0.15 m, as shown in fig. 1. The mean heat flow rate per unit length of the GHE is set as 45 W/m and 30 W/m in summer and winter, respectively. The operation period is three months no matter for summer or winter according to the practical operation. The operating cycle is from the beginning of summer cooling to the end of the winter heating. The space calculation step is set to be 0.5 m, and the time calculation step is one month. Table 1 presents the detail parameters of boreholes and soil thermal properties. The

groundwater is assumed to flow along the positive direction of  $x$ -axis, and the velocity varies over several orders of magnitude in natural aquifers [21]. The simulation is performed through the software of MATLAB, which processed the data calculated by the software of VC 6.0 based on the MFLS model.

**Analyses on the influence of advection velocity**

Supposing that both the boundary conditions and the soil thermal property parameters are constant, three different velocities of groundwater advection are selected ( $U_1 = 5 \cdot 10^{-6}$ ,  $U_2 = 5 \cdot 10^{-7}$ , and  $U_3 = 5 \cdot 10^{-8}$  m/s). Figure 2 indicates that the soil field temperature variation at different advection velocity after 20-years operation, the 3-D temperature distribution shows in the upper part and its value presents on the  $z$ -axis. It is shown that the weak heat accumulation and the low temperature are induced by the high groundwater advection velocity in the central region, which enhanced the convective heat transfer between the groundwater and boreholes, and transferred the heat to the groundwater in time to reduce the excessive temperature effectively. However, a low temperature zone appears in the soil when the advection velocity becomes high, which dues to the boreholes takes a lot of heat from the soil and

**Table 1. Parameters of boreholes and soil thermal properties**

| Parameter  | Values              |
|--|---------------------|
| Borehole spacing [m]                                 | 5                   |
| Borehole depth [m]                                   | 100                 |
| Soil thermal capacity [ $Jm^{-3}K^{-1}$ ]            | $3.0 \cdot 10^6$    |
| Soil thermal conductivity [ $Wm^{-1}K^{-1}$ ]        | 2.5                 |
| Initial temperature [K]                              | 288                 |
| Porosity   | 0.3                 |
| Advection velocity [ $ms^{-1}$ ]                     | $5.0 \cdot 10^{-7}$ |
| Groundwater thermal conductivity [ $Wm^{-1}K^{-1}$ ] | 0.587               |
| Groundwater thermal capacity [ $Jm^{-3}K^{-1}$ ]     | $4.187 \cdot 10^6$  |

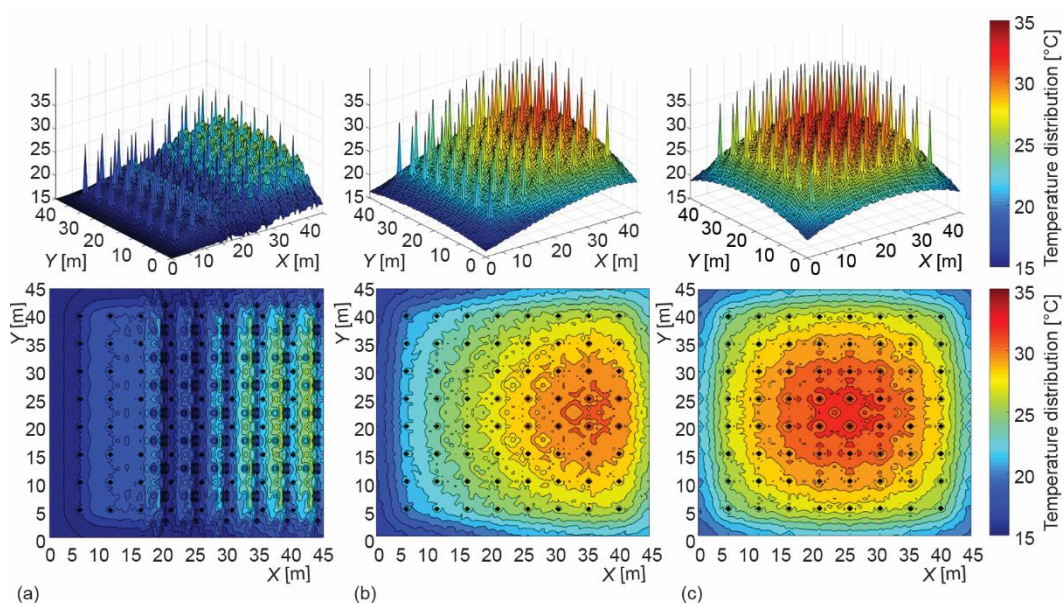


**Figure 2. Soil temperature distribution at different advection velocity; (a)  $U_1 = 5 \cdot 10^{-6}$  m/s, (b)  $U_2 = 5 \cdot 10^{-7}$  m/s, and (c)  $U_3 = 5 \cdot 10^{-8}$  m/s**

groundwater takes the heat away in time at the end of the winter heating; On the other hand, there is almost no heat accumulation and the upstream temperature is significantly lower at the end of summer cooling. Therefore, the magnitude of the advection velocity should be reasonably considered in the borehole field layout. It is noteworthy that while preventing the heat accumulation from the lower advection velocity, the faster advection velocity causes the temperature in some areas to be lower, thus diminishing the heating efficiency in winter.

### ***Analyses on the influence of soil thermal properties***

Since the heat transfer of GHE through the surrounding soil and boreholes, it is essential to study the soil thermal properties, which mainly include soil porosity, soil thermal conductivity in this section. The soil porosity  $\varphi_1 = 0.1$ ,  $\varphi_2 = 0.3$ , and  $\varphi_3 = 0.5$  were selected to study the evolution of soil temperature distribution at the advection velocity of  $U$  is  $5 \cdot 10^{-7} \text{m/s}$ . It can be observed from fig. 3 that temperature distribution only presents a small difference in the upstream and edge regions. However, the temperature difference behaves much more noticeable at the downstream center. The soil studied in this paper includes rock-soil and groundwater. Since the conductivity of rock-soil is larger and the volumetric specific heat is smaller than those of groundwater, as can be seen from the  $\lambda = \varphi\lambda_w + (1 - \varphi)\lambda_s$ , the effective thermal conductivity decreases as the porosity increases, and the effect of the heat diffusion would be worse, the heat accumulation would be increased significantly within the GHE' central area, which will result in the continuous expansion of the higher temperature area.

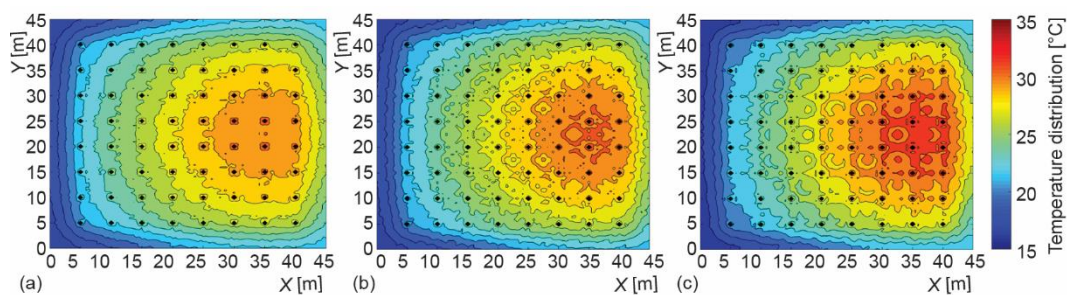


**Figure 3. Soil temperature distribution at different porosity; (a)  $\varphi_1 = 0.1$ , (b)  $\varphi_2 = 0.3$ , and (c)  $\varphi_3 = 0.5$**

In addition, the soil thermal conductivity is selected as the  $\lambda_1 = 1.5 \text{ Wm}^{-1}\text{K}^{-1}$ ,  $\lambda_2 = 2.0 \text{ Wm}^{-1}\text{K}^{-1}$ , and  $\lambda_3 = 2.5 \text{ Wm}^{-1}\text{K}^{-1}$  with other physical parameters keeping constant. The fig. 4 demonstrates that the soil temperature distribution shifts along the advection and the heat accumulates in the downstream. It can be found that the porous medium with a larger soil thermal conductivity is favorable to the heat diffusion and alleviates heat accumulation. Since the heat transfer performance is limited by the smaller soil thermal conductivity as the same advection velocity, which will cause the severe heat accumulation in the downstream. Consequently, the borehole field layout should be fully considered.

### **Research on the strategy of borehole field layouts**

#### ***Different borehole field layouts and soil parameters***

In view of the serious heat accumulation conditions with advection, effective solutions are explored through different borehole field layout. In this section, the new borehole

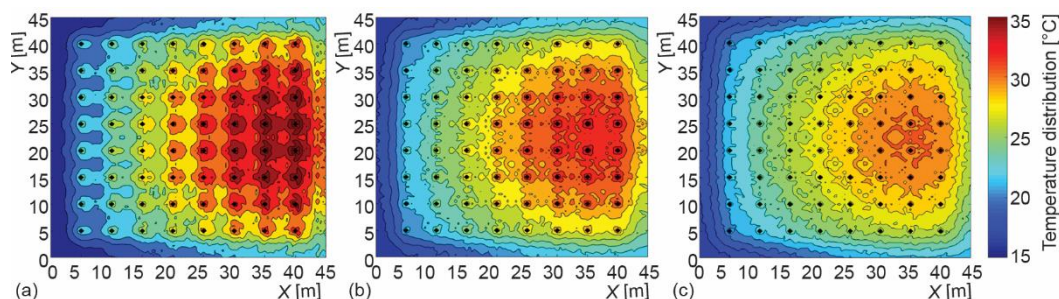


**Figure 4. Soil temperature distribution at different soil thermal conductivity;**  
 (a)  $\lambda_1 = 1.5 \text{ W/mK}$ ,  $\lambda_2 = 2.0 \text{ W/mK}$ , and  $\lambda_3 = 2.5 \text{ W/mK}$

field layout is achieved by reducing the borehole spacing from 5 m to 4 m under the condition of keeping the same amount boreholes without changing the original ground area. Keeping the heat load unchanged, nine types of borehole field layout such as *U*-shaped,  $\pi$ -shaped and circular shape are considered. According to the analysis of the soil field temperature variation, heat accumulation and enthalpy increment of GHE in different borehole field layout at the end of summer operation, the advisable layout method can be found under different geological conditions, and the corresponding layout suggestions are given. Since this section is mainly to study the effect of different borehole field layout on soil field temperature, the operation time is set to ten years to save the program calculation time as there are many borehole field layouts. The nine new kinds of borehole field layouts are named as Case 1-9, as shown in fig. 5, while the original uniform distributed borehole field layout was named Case 0. In order to understand the effect of borehole field layout on temperature distribution of different soil structures in the heat transfer of GHE, the common soil structures of clay, sand-soil, and sandstone were selected as representatives. The different soil thermal property parameters are shown in tab. 2.

**Table 2. Parameters of boreholes and the selected soil thermal properties**

| Parameter  | Clay                | Sand-soil           | Sand-stone          |
|--|---------------------|---------------------|---------------------|
| Borehole spacing [m]   | 4                   | 4                   | 4                   |
| Borehole depth [m]   | 100                 | 100                 | 100                 |
| Soil thermal capacity [ $\text{Jm}^{-3}\text{K}^{-1}$ ]            | $3.30 \cdot 10^6$   | $1.40 \cdot 10^6$   | $3.57 \cdot 10^6$   |
| Soil thermal conductivity [ $\text{Wm}^{-1}\text{K}^{-1}$ ]        | 1.5                 | 2.0                 | 3.0                 |
| Initial temperature [K]  | 288                 | 288                 | 288                 |
| Porosity   | 0.5                 | 0.2                 | 0.1                 |
| Advection velocity [ $\text{ms}^{-1}$ ]                            | $6.0 \cdot 10^{-7}$ | $4.0 \cdot 10^{-7}$ | $8.0 \cdot 10^{-7}$ |
| Groundwater thermal conductivity [ $\text{Wm}^{-1}\text{K}^{-1}$ ] | 0.587               | 0.587               | 0.587               |
| Groundwater thermal capacity [ $\text{Jm}^{-3}\text{K}^{-1}$ ]     | $4.187 \cdot 10^6$  | $4.187 \cdot 10^6$  | $4.187 \cdot 10^6$  |

***Influence of different soil structures on temperature distribution***

The soil field temperature distribution with the original uniform borehole field layout in three different geological structures were shown in fig. 6. It can be found that there is

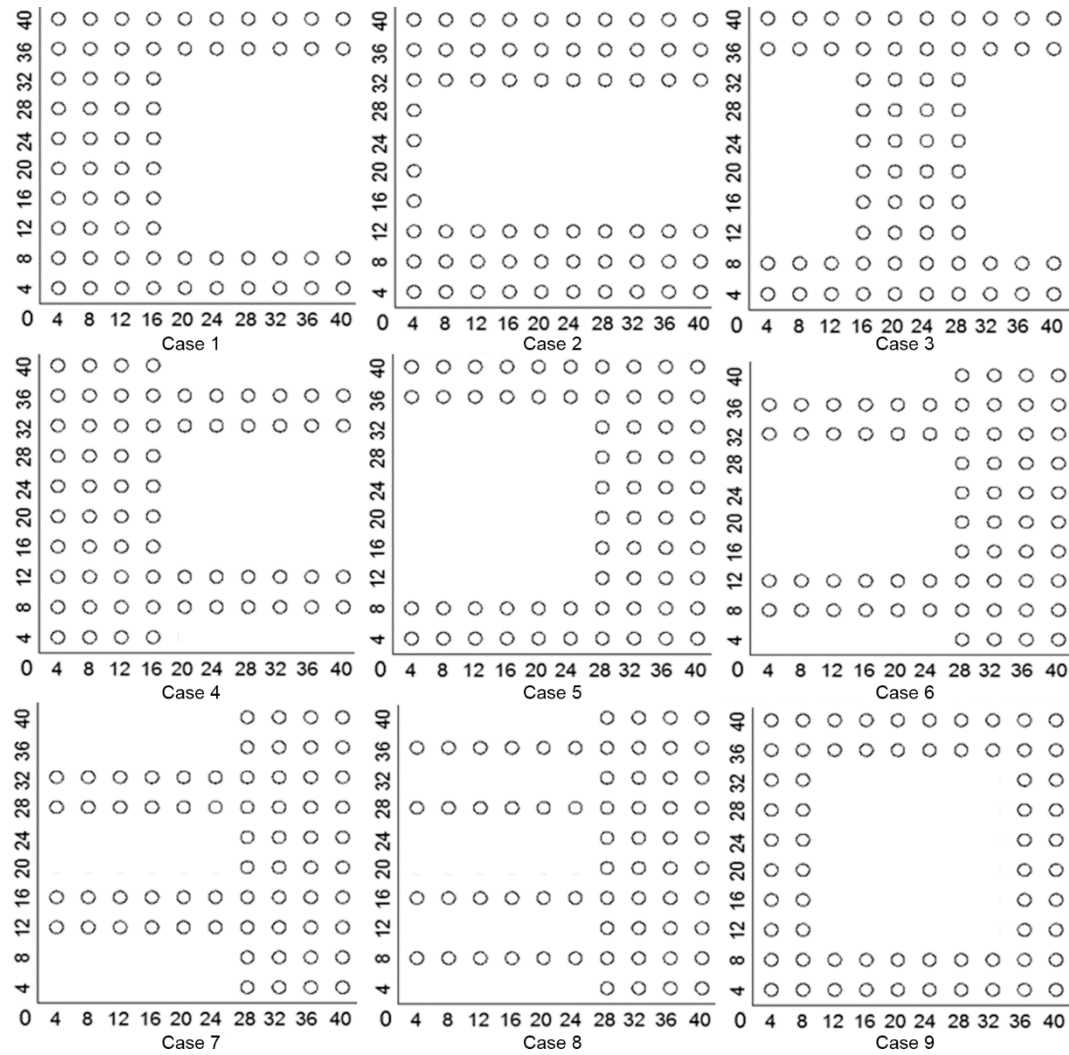


Figure 5. Nine kinds of borehole field layout

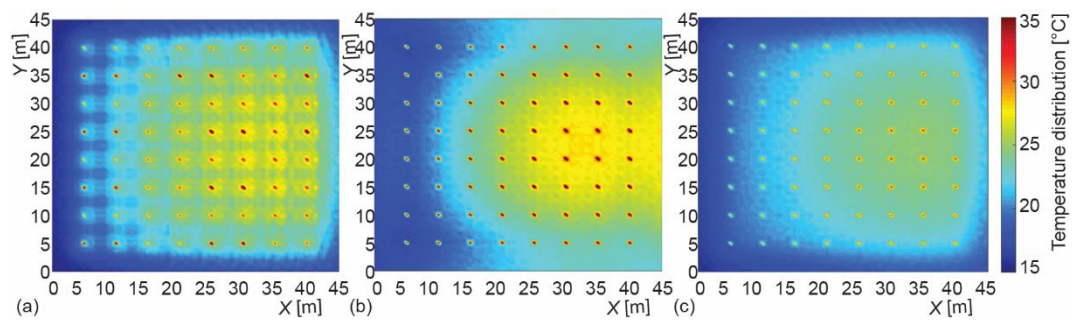


Figure 6. Temperature distribution under different geological conditions; (a) clay, (b) sand-soil, and (c) sand-stone

nearly no heat accumulation because the excessive heat can be rejected in time when the thermal conductivity and advection velocity of are larger, such as that in the sand-stone geological condition. However, low temperature in the upstream region will also affect the heating efficiency of GHE in winter with high advection velocity. As for the clay with the smaller thermal diffusion coefficient and advection velocity, the overall soil field temperature is higher as excessive heat cannot be rejected in time. Moreover, the average soil field temperature increment of the sand-soil structure with the higher thermal diffusivity between the clay and sand-stone, which means that the gradient of the soil field temperature distribution is increased with the smaller heat resistance of sand-soil. As a result, this induces the heat accumulation severely in the advection downstream and serious decline in the performance of GHE. Therefore, it is significant to find a reasonable method to solve the series of the problems including the thermal anomalies and heat accumulation during operation, and the new borehole field layout is a simple way to deal with these challenges in practice.

Here, the enthalpy increment of soil field is introduced in order to further analyze the heat accumulation with different borehole field layout, and thus the severity of the temperature distribution change was characterized. The enthalpy increment in soil temperature field is:

$$\Delta H = (\rho c)_{\text{por}} \frac{V \Delta T}{1000} \quad (9)$$

$$V = SL \quad (10)$$

where  $\Delta H$  [kJ] is the enthalpy increment,  $V$  [m<sup>3</sup>] – the soil heat exchange volume, and  $\Delta T$  [°] – the average soil field temperature increment at the end of the summer operation. According to eq. (9), the soil enthalpy increment with operation time can be obtained, as shown in fig. 7.

#### Clay geological condition

The soil field temperature distribution and heat accumulation of multi-boreholes with clay geological conditions in different borehole field layout is demonstrated in fig. 8. As for the traditional uniform layout, the higher soil temperature region is obviously larger since the thermal conductivity and thermal diffusivity of the clay are smaller, and the heat accumulation easily occurs as the operation extended. It is well known that the heat transfer process around the boreholes is a coupled process of heat conduction through the soil and water in its pores and heat convection by moving groundwater. Due to the higher groundwater advection velocity in the clay structure, the heat transfer mode is mainly dominated by the convective heat transfer of groundwater, which results in ineffective heat diffusion and severe heat accumulation in the downstream as the relatively small thermal conductivity with advection. It can be seen from Cases 1, 3, and 5 in fig. 8 that the borehole field layout concentrates relatively in the groundwater advection downstream, which can reduce the area the higher temperature region and the heat accumulation effectively in the smaller thermal conductivity and thermal

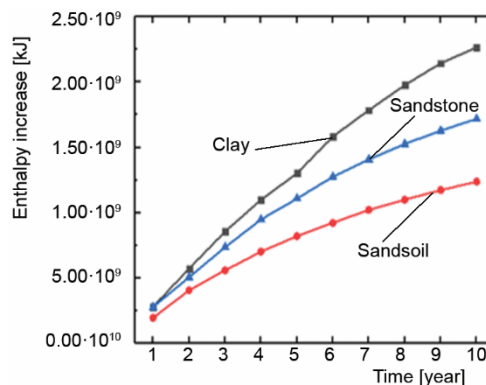


Figure 7. The enthalpy increment under different geological conditions

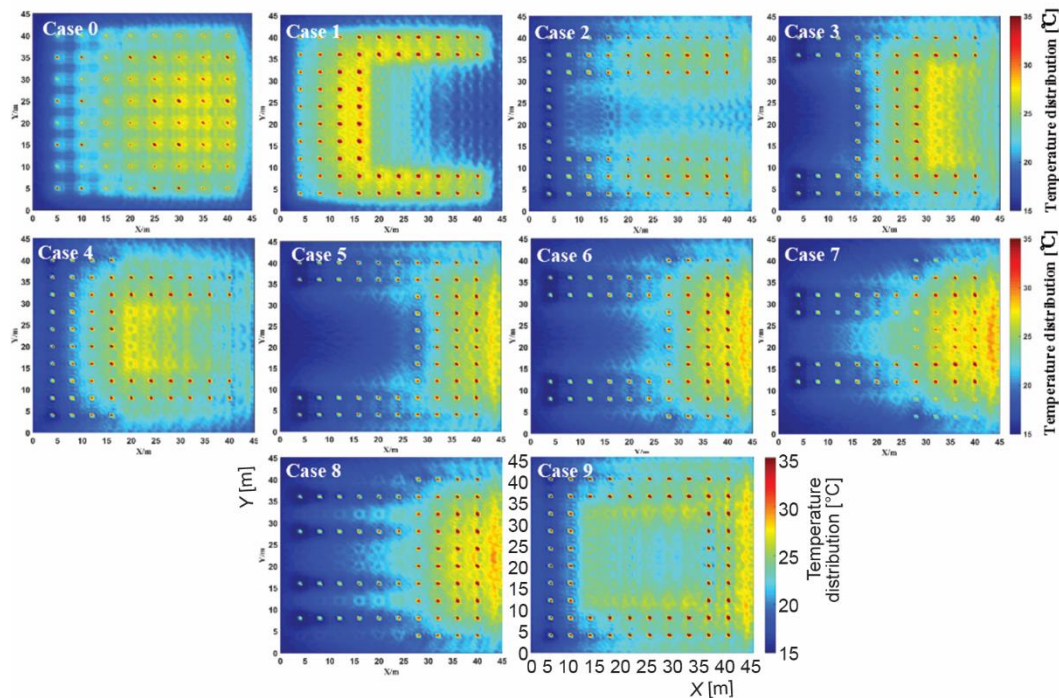


Figure 8. Temperature distribution of different pipe layouts in clay

diffusivity geological condition. Because the heat generated decreases as the number of upstream pipes decreases, there is enough time for the heat to diffuse to diminish the heat accumulation. It can be seen from the Cases 5-8 in fig. 8 that the more boreholes are dispersed relative along the advection center line, the less heat accumulation occurs, which means the thermal interference can be weakened between the boreholes, which is benefit for the heat diffusion to avoid heat accumulation. Moreover,

the comparison between the Case 2 and Case 5 indicates that the more boreholes on both sides the higher temperature area occurs.

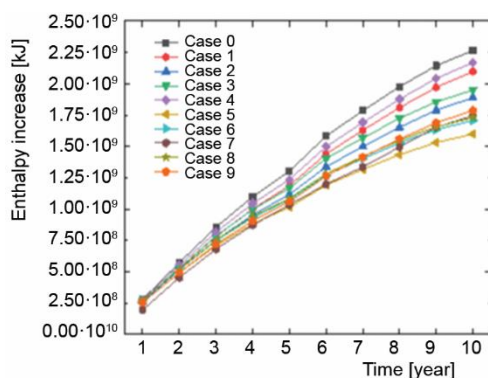


Figure 9. Enthalpy increment of different pipe layouts in clay

In addition, fig. 9 shows that the overall average soil enthalpy increase is significantly less than that with new borehole field layout. It also indicates that the boreholes dispersed relative to the advection centerline is benefit to decrease the soil field enthalpy increment in Cases 5-9. The higher soil enthalpy means more heat accumulates as the lower thermal diffusivity of the clay structure, which will reduce the operation life of GHE in the region. Thus, the Cases 1-4 may not be the good choices. Considering the soil field higher temperature region and heat accumulation in previous analysis, it is better to configure the borehole concentrated

relatively in the groundwater advection downstream and dispersed relatively along the advection centerline to effectively prevent the heat accumulation in the geological condition which the thermal conductivity and thermal diffusivity are both smaller.

*Sand-soil geological condition*

Figure 10 presents that the temperature field variation of sand-soil is more significant as the result of the lower advection velocity, the higher thermal diffusion coefficient and thermal conductivity. In this case, the thermal migration is mainly dominated by the soil thermal conduction. The higher thermal diffusion coefficient and the smaller specific heat induce the higher temperature region extension and serious heat accumulation in the advection downstream, which are caused by slow soil temperature recovery. In the new borehole field layouts, fig. 11 indicates that the average enthalpy increment of the sand-soil is also reduced significantly, especially in Cases 5 and 9, where the heat accumulation is weaker. As for the geological environment where the sand-soil presents a smaller thermal conductivity and a larger thermal diffusivity, the heat accumulation problem is the most prominent. The borehole field layout should be distributed along the advection to both sides as much as possible to reduce the heat accumulation effect. However, the heat accumulation of Case 5 is more serious than that of Case 9 so that the boreholes near the end of the groundwater advection may diminish heat transfer performance at first, the Case 9 maybe a better choice.

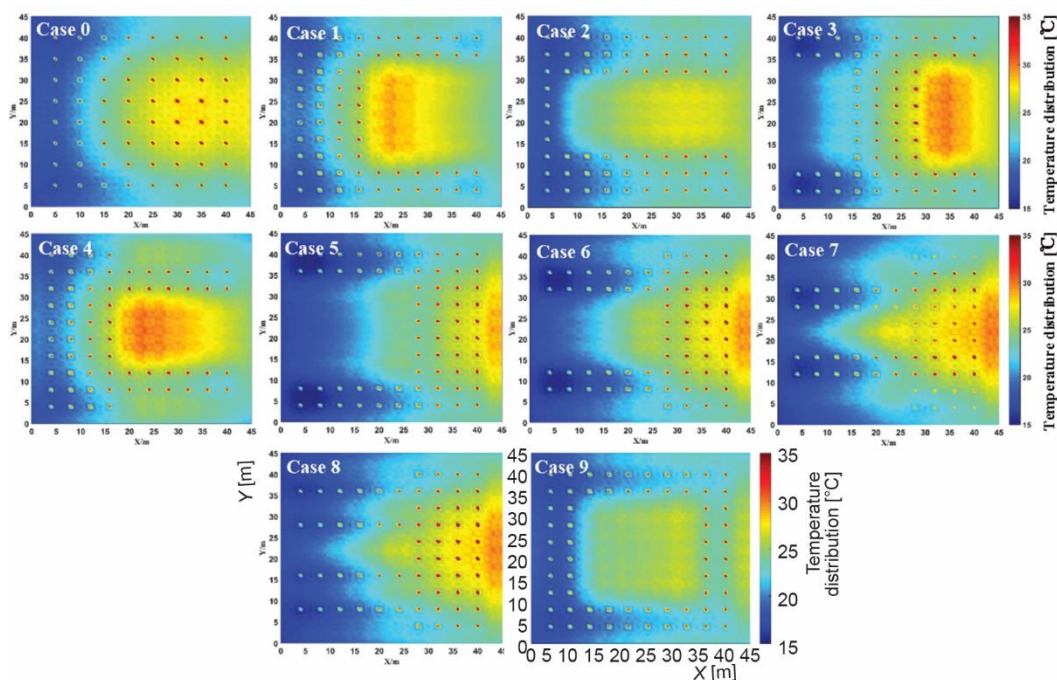
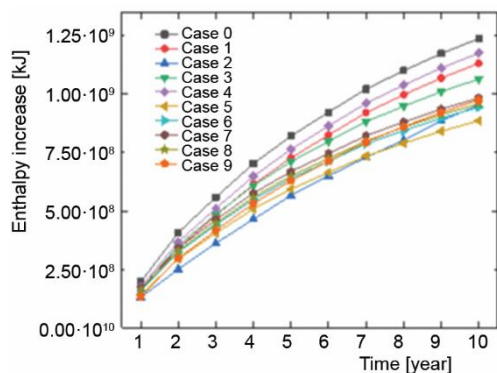


Figure 10. Temperature distribution of different pipe layouts in sand-soil

*Sand-stone geological condition*

The soil field temperature distribution of fig. 12 indicates that the excessive heat can be rejected in time due to the higher advection velocity and thermal conductivity of the sand-



**Figure 11. Enthalpy increment of different pipe layouts in sand-soil**

and compares the soil temperature distribution and enthalpy increment of nine kinds of borehole field layouts in three kinds of soil with those of the normal uniform layout. The main conclusions are as following.

stone. The average soil temperature is lower and the global heat transfer performance is better as a result of negligible heat accumulation. The soil enthalpy increment given in fig. 13 denotes the Case 5 is the smallest and can be stabilized earlier. For the geological environment with larger thermal conductivity and larger advection velocity, it is reasonable to choose the Case 5 with the smallest enthalpy increment and there is almost no heat accumulation.

**Conclusions**

The present work analyzes the effect of the soil thermal parameters and groundwater velocity on the ground temperature variation of boreholes field with unbalanced seasonal load,

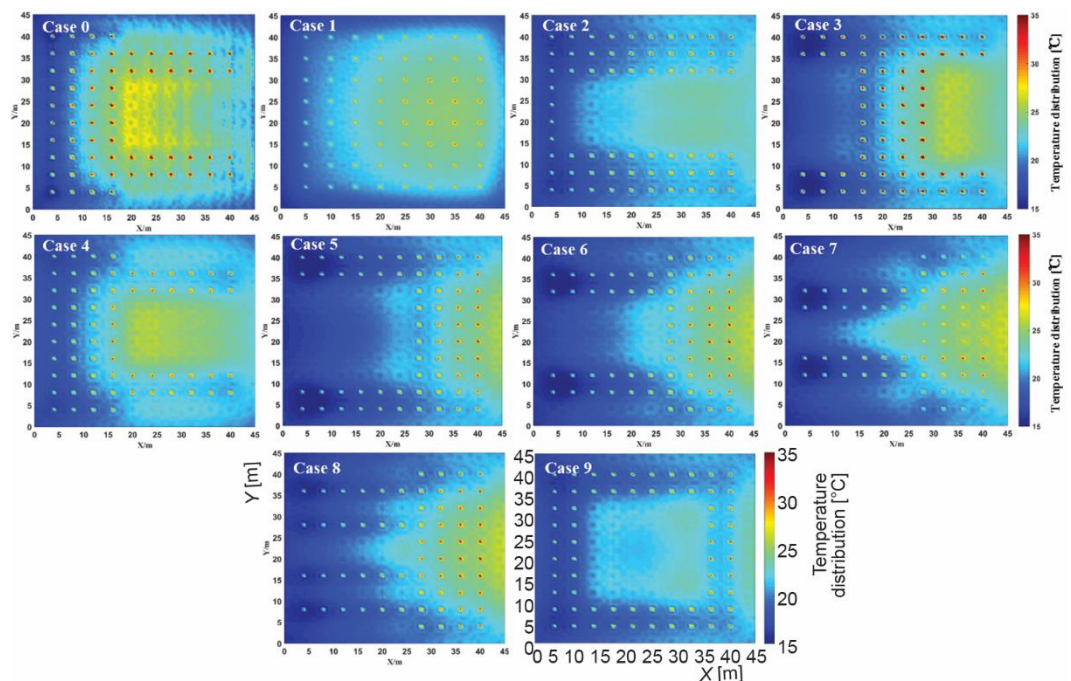


**Figure 12. Temperature distribution of different pipe layouts in sand-stone**

The increase of groundwater velocity and thermal conductivity, and the decrease of porosity reduces the highest and average soil temperature, which means the thermal accumulation is to be alleviated effectively.

The comparisons of the overall soil temperature distribution and enthalpy increment in three soil structures indicate that, the new borehole layouts by reducing the pipes spacing, which concentrated relatively in the groundwater advection downstream and dispersed relatively along the advection centerline can diminish the higher ground temperature and the heat accumulation effectively, and the effect of decreasing enthalpy increment significantly as the operation time extended in comparison with the normal uniform layout. As for the specific soil structures, with smaller soil thermal conductivity or slower groundwater advection velocity, which is advisable to configure the pipes as far as possible on both sides of the advection center line; with the faster groundwater advection velocity, adopting a circular borehole field layout is also efficient in reducing the thermal accumulation in the multi-boreholes field.

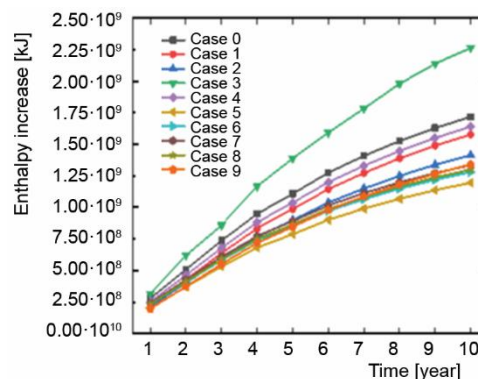


Figure 13. Enthalpy increment of different pipe layouts in sand-stone

### Acknowledgment

The work was supported by the National Key R&D Program (2019YFB1504004), Leading Researcher Studio Fund of Jinan (2019GXRC066) and the Shandong Provincial Natural Science Foundation (ZR2017MEE037).

### Nomenclature

$c$  – specific heat capacity, [ $\text{Jkg}^{-1}\text{K}^{-1}$ ]  
 $\Delta H$  – enthalpy increment, [kJ]  
 $L$  – borehole depth, [m]  
 $r$  – radial co-ordinate, [m]  
 $q_l$  – borehole heat transfer rate per unit length, [ $\text{Wm}^{-1}$ ]  
 $S$  – borehole cross-area, [ $\text{m}^2$ ]  
 $T_0$  – initial temperature, [K]  
 $u$  – advection velocity, [ $\text{ms}^{-1}$ ]  
 $x, y, z$  – cartesian co-ordinates, [m]

### Greek symbols

$\alpha$  – thermal diffusivity, [ $\text{m}^2\text{s}^{-1}$ ]  
 $\lambda$  – thermal conductivity, [ $\text{Wm}^{-1}\text{K}^{-1}$ ]  
 $\rho$  – density, [ $\text{kgm}^{-3}$ ]  
 $\tau$  – time, [s]  
 $\phi$  – ground porosity

### Subscripts

s – solid  
 w – water

### References

- [1] Aresti, L., et al., A Review of the Design Aspects of Ground Heat Exchangers, *Renewable & Sustainable Energy Reviews*, 92 (2018), 2, pp. 757-773
- [2] Pouloupatis, P., et al., Measurements of Ground Temperatures in Cyprus for Ground Thermal Applications, *Renewable Energy*, 36 (2011), 2, pp. 804-814
- [3] Sivasakthivel, T., et al., Experimental Thermal Performance Analysis of Ground Heat Exchangers for Space Heating and Cooling Applications, *Renewable Energy*, 113 (2017), 5, pp. 1168-1181
- [4] Luo, J., et al., Heating and Cooling Performance Analysis of a Ground Source Heat Pump System in Southern Germany, *Geothermics*, 53 (2015), 11, pp. 57-66
- [5] Zhai, X. Q., et al., Heating and Cooling Performance of a Minitype Ground Source Heat Pump System, *Applied Thermal Engineering*, 111 (2017), 2, pp. 1366-1370
- [6] Lazzari, S., et al., Long-Term Performance of BHE (Borehole Heat Exchanger) Fields with Negligible Groundwater Movement, *Energy*, 35 (2010), 12, pp. 4966-4974

- [7] Zhang, J. J., *et al.*, Effect of a Cumulative Cold and Heat Load Ratio on Hybrid Ground-Source Heat Pump System Performance Parameters, *Advanced Materials Research*, 1092 (2015), 1, pp. 26-35
- [8] Ali, M., Modelling the Performance of Horizontal Heat Exchanger of Ground-Coupled Heat Pump System with Egyptian Conditions, Ph. D. thesis, University of Manchester, Manchester, UK, 2013
- [9] Sivasakthivel, T., *et al.*, Optimization of Ground Heat Exchanger Parameters of Ground Source Heat Pump System for Space Heating Applications, *Energy*, 78 (2014), 2, pp. 573-586
- [10] Zhang, L., *et al.*, Analyses on Soil Temperature Responses to Intermittent Heat Rejection from BHEs in Soils with Groundwater Advection, *Energy and Buildings*, 107 (2015), 2, pp. 355-365
- [11] Spittler, J. D., *et al.*, Natural Convection in Groundwater-Filled Boreholes Used as Ground Heat Exchangers, *Applied Energy*, 164 (2016), 5, pp. 352-365
- [12] Luo, J., *et al.*, Influence of Groundwater Levels on Effective Thermal Conductivity of the Ground and Heat Transfer Rate of Borehole Heat Exchangers, *Applied Thermal Engineering*, 128 (2018), 2, pp. 508-516
- [13] Erol, S., *et al.*, Multilayer Analytical Model for Vertical Ground Heat Exchanger with Groundwater Flow, *Geothermics*, 71 (2018), 2, pp. 294-305
- [14] Kurevija, T., *et al.*, Effect of Borehole Array Geometry and Thermal Interferences on Geothermal Heat Pump System, *Energy Conversion and Management*, 60 (2012), 2, pp. 134-1
- [15] Pu, L., *et al.*, Structure Optimization for Horizontal Ground Heat Exchanger, *Applied Thermal Engineering*, 136 (2018), 1, pp. 131-140
- [16] Xu, L., *et al.*, Influences of Structure Parameters on Performance of Tree-Shaped Ground Heat Exchanger, *Energy Procedia*, 158 (2019), 3, pp. 5954-5961
- [17] Gunawan, E., *et al.*, Alternative Heating Systems for Northern Remote Communities: Techno-economic Analysis of Ground-Coupled Heat Pumps in Kuujuaq, Nunavik, Canada, *Renewable Energy*, 147 (2020), 2, pp. 1540-1553
- [18] Bryś, K., *et al.*, Characteristics of Heat Fluxes in Subsurface Shallow Depth Soil Layer as a Renewable Thermal Source for Ground Coupled Heat Pumps, *Renewable Energy*, 146 (2020), 1, pp. 1846-1866
- [19] Mingzhi, Y., *et al.*, Zoning Operation of Multiple Borehole Ground Heat Exchangers to Alleviate the Ground Thermal Accumulation Caused by Unbalanced Seasonal Load, *Energy and Buildings*, 110 (2015), 1, pp. 345-352
- [20] Molinagiraldo, N., *et al.*, A Moving Finite Line Source Model to Simulate Borehole Heat Exchangers with Groundwater Advection, *International Journal of Thermal Sciences*, 50 (2011), 12, pp. 2506-2513
- [21] Capozza, A., *et al.*, Investigations on the Influence of Aquifers on the Ground Temperature in Ground-Source Heat Pump Operation, *Applied Energy*, 107 (2013), 11, pp. 350-363
- [22] Song, X., *et al.*, Numerical Analysis of Heat Extraction Performance of a Deep Coaxial Borehole Heat Exchanger Geothermal System, *Energy*, 164 (2018), 5, pp. 1298-1310
- [23] Li, C., *et al.*, Numerical Simulation of Ground Source Heat Pump Systems Considering Unsaturated Soil Properties and Groundwater Flow, *Applied Thermal Engineering*, 139 (2018), 2, pp. 307-316
- [24] Choi, J. C., *et al.*, Numerical Evaluation of the Effects of Groundwater Flow on Borehole Heat Exchanger Arrays, *Renewable Energy*, 52 (2013), 3, pp. 230-240
- [25] Fan, R., *et al.*, A Study on the Performance of a Geothermal Heat Exchanger Under Coupled Heat Conduction and Groundwater Advection, *Energy*, 32 (2007), 11, pp. 2199-2209
- [26] Molina-Giraldo, N., *et al.*, A Moving Finite Line Source Model to Simulate Borehole Heat Exchangers with Groundwater Advection, *International Journal of Thermal Sciences*, 50 (2011), 12, pp. 2506-2513
- [27] Boon, D., *et al.*, Groundwater Heat Pump Feasibility in Shallow Urban Aquifers: Experience from Cardiff, UK, *Science of The Total Environment*, 697 (2019), 10, pp. 133847-133847
- [28] Rybach, B. *et al.*, Geothermal Heat Pump Development: Trends and Achievements in Europe. Perspectives for Geothermal Energy in Europe, in: *Perspectives for Geothermal Energy in Europe*, (ed. R. Bertani), Enel Green Power, Rome, Italy, 2017, Chapter 7, pp. 215-253